

Effect of CO gas and anode-metal loading on H₂ oxidation in proton exchange membrane fuel cell

Jae-Dong Kim^{*}, Yong-Il Park, Koichi Kobayashi, Masayuki Nagai

Advanced Research Center for Energy and Environment, Musashi Institute of Technology, 1-28-1 Tamazutsumi, Setagaya-ku, Tokyo 158-8557, Japan

Received 19 March 2001; accepted 12 June 2001

Abstract

The effect of CO gas and anode-metal loading on H₂ oxidation in a proton exchange membrane fuel cell (PEMFC) are investigated by ac impedance spectroscopy. To investigate these effects, the voltage loss is measured, and the impedance of the half-cell (cathode side: H₂; anode side: simulated gas) and full-cell (cathode side: O₂; anode side: simulated gas) are determined by ac impedance spectroscopy. The CO gas has a great effect on the charge-transfer reaction (high-frequency arc) and hydrogen dissociative chemisorption (medium-frequency arc), but little effect on the low-frequency arc. The polarization resistances for charge-transfer and hydrogen dissociative chemisorption in a fuel cell with low metal loading are larger than those with high metal loading, and increase greatly with increasing CO concentration. Although the cathode impedance is the main part at high temperature irrespective of CO concentration (≤ 100 ppm), the impedance of the full-cell depends on anode impedance at low temperature and high CO concentration. © 2001 Elsevier Science B.V. All rights reserved.

Keywords: Proton exchange membrane fuel cell; Impedance spectroscopy; Polarization resistance; H₂ oxidation; Metal loading; Carbon monoxide

1. Introduction

The proton exchange membrane fuel cell (PEMFC) which uses hydrogen as a fuel is regarded as highly attractive for mobile applications due to its high power density in the temperature range 60–100°C [1]. Methanol shows some advantages compared with liquid or compressed hydrogen in terms of weight, volume, and range [2]. For such a fuel cell system to use hydrogen derived from methanol, a reformer is required. The reformer converts methanol to a hydrogen-rich fuel gas which contains about 75% H₂, 24% CO₂ and 1% CO [3,4]. Although platinum is known to be one of the most effective catalysts for hydrogen oxidation in a PEMFC, there are problems when the fuel gas contains CO. Even a few parts per million of CO cause poisoning of the platinum and this results in a substantial degradation in the performance of the fuel cell [5,6]. On the other hand, it has been reported that Pt–Ru alloy is a promising electrocatalyst for the oxidation of adsorbed CO [7–9]. Furthermore, other workers [10,11] have demonstrated that a number of elements exhibit a co-catalytic activity for the anodic oxidation of CO. All these results have been obtained, however, at smooth platinum or platinum alloy electrodes in an aqueous sulfuric acid. Therefore, we have

studied the effect of CO gas and anode-metal loading on H₂ oxidation in a PEMFC.

2. Experimental

The fuel cell tested was a 1 cm² single cell which employed a Nafion 115 membrane (Aldrich). The membrane was pretreated by boiling for 1 h in each step in 3% H₂O₂, distilled water, 0.5 M H₂SO₄, and again distilled water. A carbon-supported electrocatalyst (Pt/C, 46.8 wt.% Pt) (Tanaka Kikinzoku Kogyo K.K.) and a carbon-supported electrocatalyst (atomic ratio Pt 0.4–Ru 0.6/C, 54 wt.% Pt–Ru) (Tanaka Kikinzoku Kogyo K.K.) were used as the cathode and the anode, respectively. To prepare the catalyst ink mixture, 5% Nafion solution (Aldrich) was added to the water-wetted catalysts. To prepare the membrane/electrode assembly (MEA), the anode and the cathode inks were uniformly painted on to two PTFE-treated carbon papers. In the MEA, the metal loading of the cathode was 0.4 mg cm⁻² and the metal loading of anode was 0.84 mg cm⁻² (high metal loading) or 0.4 mg cm⁻² (low metal loading). The Nafion loading of the anode was 0.62 mg cm⁻² (high metal loading) or 0.29 mg cm⁻² (low metal loading). In all experiments, oxygen and simulated gas were prehumidified at 5 and 15°C higher than the cell temperature, respectively. The humidified O₂ was fed into

^{*} Corresponding author. Fax: +81-3-5705-2163.
E-mail address: nature88@hanmail.net (J.-D. Kim).

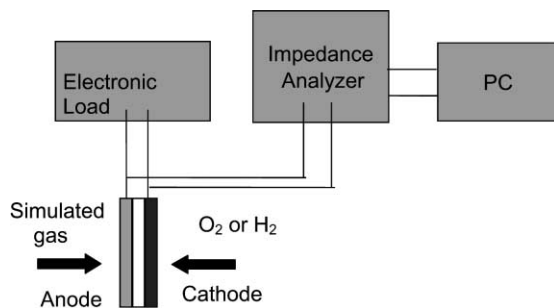


Fig. 1. Experimental set-up for impedance measurements.

the cathode compartment at 500 sccm. A simulated gas, i.e. 60% H_2 /20% CO_2 /20% N_2 with 0 ppm CO or 60% H_2 /20% CO_2 /20% N_2 with various CO concentrations (30, 60 and 100 ppm), was fed into the anode compartment at 500 sccm. The gas of composition 60% H_2 /20% CO_2 /20% N_2 with 0 ppm CO was used as a reference to compare the voltage loss and change of polarization of the fuel cell. The fuel cells were operated at cell temperatures of 30, 50 and 70°C with pressures in the anode and cathode compartments of 1 atm. Since CO poisoning of anode required a certain period of time, the voltage loss and impedance of the fuel cell were measured after the voltage of fuel cell was stable. The poisoning time increased with decrease in cell temperature and a few hours were required at 30°C. Air bleeding was used before changing simulated gas.

The ac impedance measurements were performed by means of an impedance analyzer (ZAHENR, Model IM6e), and were conducted under pseudo-galvanostatic or potentiostatic control of the cell over the frequency range 15 kHz to 10 MHz. A small ac signal 10 mV in amplitude was used to perturb the system throughout the experiments. A schematic diagram of the experimental set-up employed for measuring the impedance is shown in Fig. 1.

3. Results and discussion

In order to investigate the effect of CO concentration on the performance of the fuel cell, the cell potential was measured at a current density of 300 mA cm^{-2} by varying the CO concentration. The voltage loss of the fuel cell was calculated by subtracting the cell potential at each CO concentration from the cell potential at 0 ppm CO concentration. The results are shown in Fig. 2. The voltage loss of the cell is found to increase slightly with increasing CO and is inversely proportional to the amount of anode-metal loading.

In order to clarify the effect of CO gas on the impedance of PEMFC, two methods were attempted for measuring impedance. First, impedance measurements were carried out in the half-cell condition (cathode: H_2 ; anode: simulated gas). Second, the impedance measurements were conducted in the full-cell condition (cathode: O_2 ; anode: simulated gas). When the impedance of the full-cell is measured, the

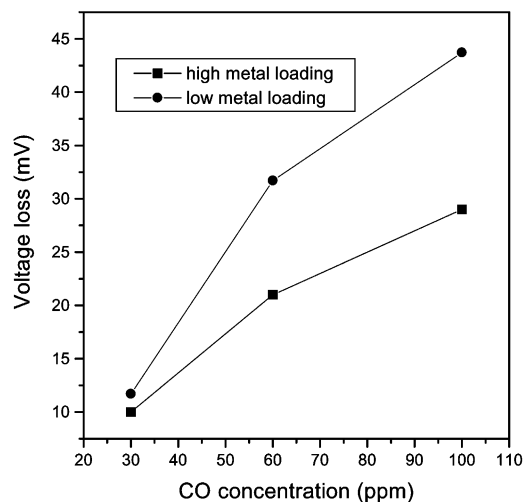


Fig. 2. Voltage loss as a function of CO concentration.

impedance spectra give the information about cathode and anode impedance. The impedance spectra of the full-cell are nearly equal to the cathode impedance because the hydrogen oxidation reaction is very fast. It is possible to eliminate the contribution of the cathode by operating the PEMFC with a continuous stream of hydrogen in the cathode [12]. The results of the half-cell are shown in Fig. 3. In this case, the impedance measurement were carried out at 50°C. Three depressed arcs are observed on the impedance spectrum. In order to explain this spectrum, the equivalent circuit as shown in Fig. 3 is applied. Here, L is an inductance and R_1 represents an ohmic resistance. (R_2Q_2), (R_3Q_3) and (R_4Q_4) represent the high-frequency, the medium-frequency, and the low-frequency arc, respectively. As can be seen in Fig. 3, the measured values are in good agreement with the fitted values. The inductance can be attributed to the lead

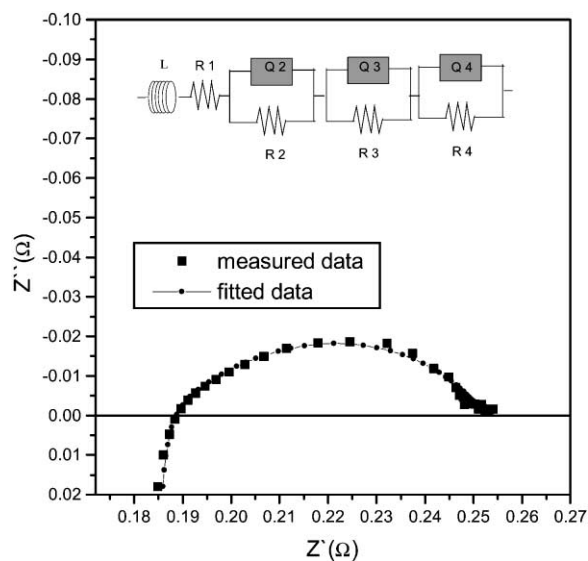
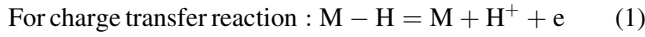
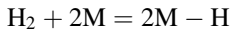


Fig. 3. Impedance spectrum for a half-cell. The impedance measurement was made at 50°C and with simulated gas (0 ppm CO)/ H_2 as reactant gas.

wires, and its value is about 210 nH. R_1 is the dc component and includes the membrane resistance. According to Ciuranu and Wang [13], the high-frequency arc (R_2Q_2) is assigned to the charge-transfer reaction at the interface and the medium-frequency arc (R_3Q_3) is assigned to hydrogen dissociative chemisorption at the electrode. If M is a vacant active site in the anode and MH is an adsorbed site, the charge-transfer reaction and the dissociative chemisorption reaction of hydrogen are given by



For hydrogen-dissociative chemisorption reaction :



The adsorbed CO changes to CO_2 above a critical potential and results in an inductive arc in the low-frequency region. The inductive arc does not appear because the experiment was performed at the open-circuit potential (OCP). When the impedance of the fuel cell was measured

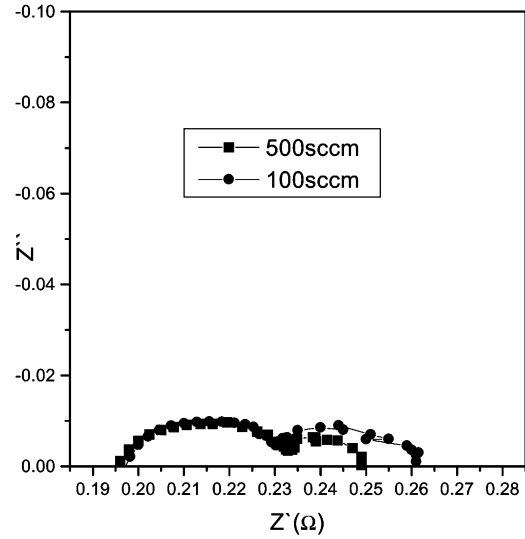


Fig. 4. Flow-rate dependence on impedance spectra.

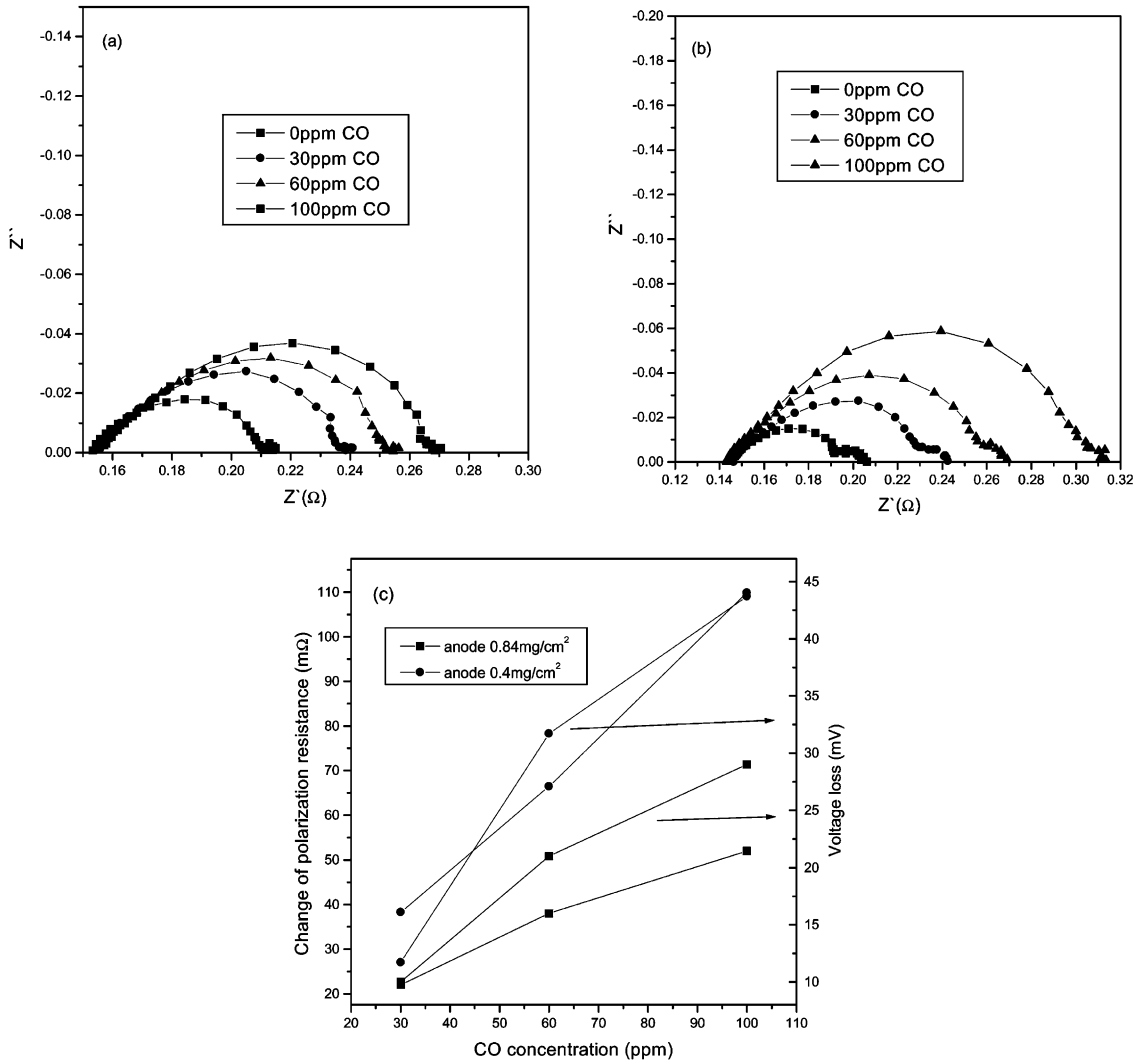


Fig. 5. Impedance spectra of half-cell with (a) high, (b) low metal loading, and (c) change of polarization resistance and voltage loss as a function of CO concentration at 70°C.

under load, a potential occurs and, for the same current, increases with decrease in cell temperature. The inductive arc appears in the impedance spectra when the impedance is measured at a current density above 200 mA cm^{-2} and a cell temperature of 30°C . This is because the critical potential is reached when adsorbed CO is converted to CO_2 . Further studies are required to define the role of CO oxidation on a Pt–Ru electrode.

The change of impedance spectra with flow rate is shown in Fig. 4. As the flow rate decreases, the high-frequency and medium-frequency arcs show little variation, but the low-frequency arc is increased markedly. This means that the low-frequency arc is due to gas-phase diffusion of hydrogen.

Impedance spectra of the half-cell as a function of CO concentration are shown in Fig. 5. The impedance spectra were measured at the OCP. The results for a fuel cell with high metal loading and low metal loading are given in Fig. 5(a) and (b), respectively. The polarization resistance increases with increasing CO concentration. In case of 0 ppm CO, the anode polarization resistance of a fuel cell

with low metal loading is smaller than that of one with a high metal loading. The change of polarization resistance of the fuel cell with low metal loading is larger than that of one with high metal loading. The voltage loss and change of polarization resistance as a function of CO concentration are shown in Fig. 5(c). In this case, the change of polarization resistance is obtained by subtracting the polarization resistance at 0 ppm CO from that at each CO concentration. The voltage losses are consistent with the change of polarization resistance. This is explained by the fact that the increase of polarization resistance in the anode side is responsible for the voltage loss.

To identify the effect of CO concentration on each reaction of the anode, the impedance spectra in Fig. 5 were analyzed by using equivalent circuit shown in Fig. 3. The results for R_2 (charge-transfer), R_3 (hydrogen dissociative chemisorption) and R_4 (hydrogen phase diffusion) are shown in Fig. 6(a)–(c), respectively. The values of R_2 and R_3 increase with increasing CO concentration, while R_4 remains constant. When H_2 containing CO is fed into the

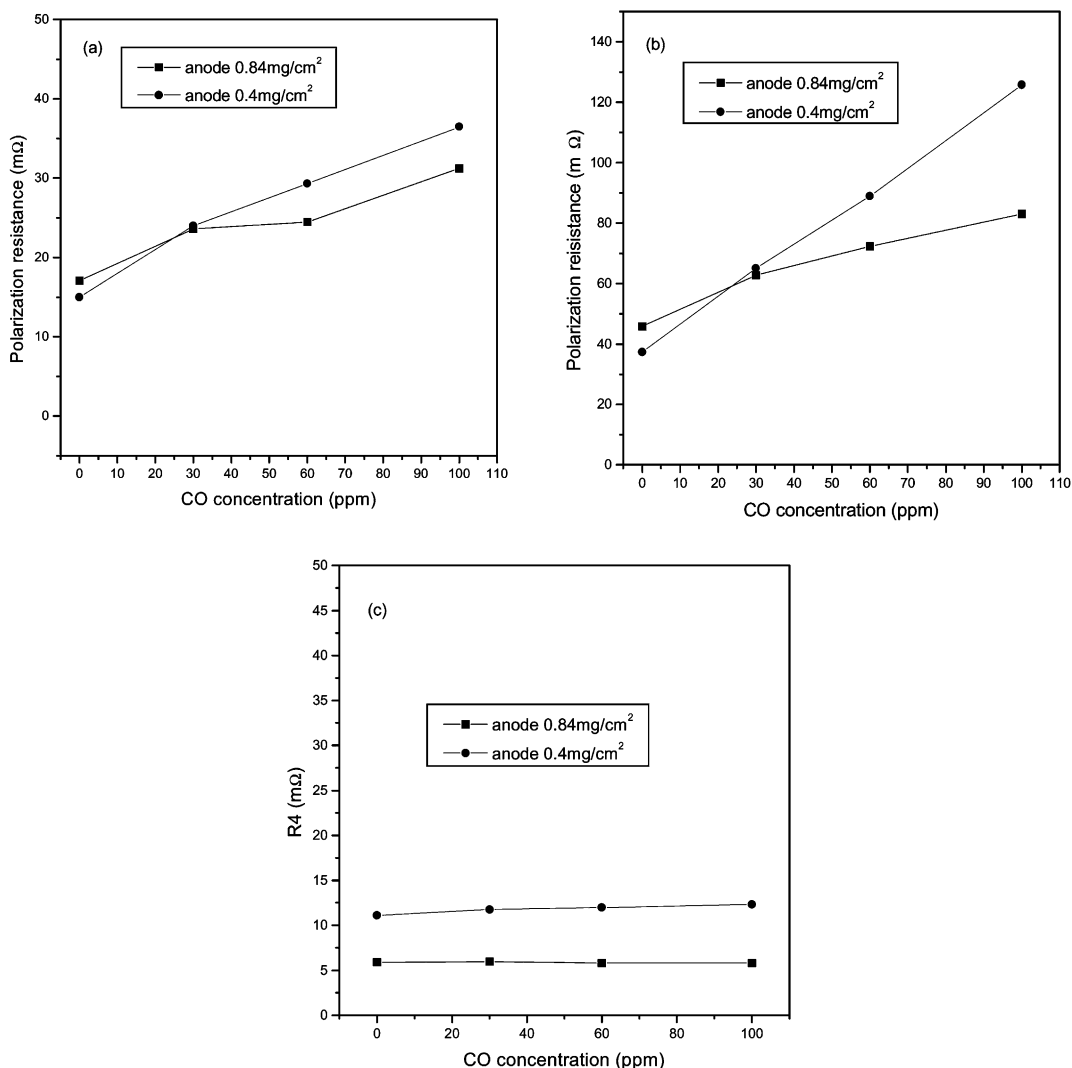


Fig. 6. Polarization resistance as a function of CO concentration: (a) R_2 ; (b) R_3 ; (c) R_4 .

anode, the H₂ gas competes with the CO gas for adsorption on the active sites. Although the CO adsorption step depends on the catalyst nature, for Pt–Ru/C free side attack is preferred instead of replacement [14]. The fraction (θ_{M-H}) of the site occupied by hydrogen is given by:

$$\theta_{M-H} = 1 - \theta_{CO} - \theta_M \quad (3)$$

where θ_{CO} is the fraction of site adsorbed with CO and θ_M the fraction of the vacant active site. Since θ_{CO} increases with increasing CO concentration, θ_{M-H} decreases with increasing CO concentration. As the rate of the charge-transfer reaction is proportional to the amount of the site occupied by hydrogen, the polarization resistance of the charge-transfer reaction increases with increasing CO concentration. According to Vogel et al. [15], the rate of hydrogen dissociative chemisorption is proportional to the fraction of the vacant site (θ_M). Since the number of vacant sites decreases with increasing CO concentration, the polarization resistance of hydrogen dissociative chemisorption increases with increasing CO concentration. The polarization resistance of hydrogen phase diffusion is given in Fig. 6(c). As the hydrogen phase diffusion is related to the supply of hydrogen, this arc changes with the porosity of the backing layer and the flow rate. Therefore, the polarization resistance of hydrogen phase diffusion is nearly constant, irrespective of CO concentration. Although the polarization resistance for 0 ppm CO in a fuel cell with low metal loading is smaller than that in one with high metal

loading, the polarization resistance for a CO-containing fuel in a fuel cell with high metal loading is smaller than that in one with low metal loading. These results are consistent with the voltage loss data shown in Fig. 2. The differences of polarization resistance and voltage loss due to metal loading are considered to be related to the amount of vacant active sites. As these sites (M) increase, the rate of the hydrogen dissociative chemisorption reaction increases and results in a decrease in the change of R_3 . Also, the amount of M–H increases. Since the charge-transfer reaction is facilitated by increase of M–H, the change in R_2 decreases. The slopes ($\Delta R/\Delta \text{ppm}$) of Fig. 6(a) are 0.13 (anode 0.84 mg cm⁻²) and 0.22 (anode 0.4 mg cm⁻²) and the slopes ($\Delta R/\Delta \text{ppm}$) of Fig. 6(b) are 0.36 (anode 0.84 mg cm⁻²) and 0.88 (anode 0.4 mg cm⁻²). From measurements of the slope of polarization resistance with CO concentration, the polarization resistance of a fuel cell with low metal loading is found to increase more than that of one with high metal loading, and the polarization resistance of hydrogen dissociative chemisorption to increase more than that of the charge-transfer reaction.

In order to check the cathode impedance in the full-cell and the effect of cell temperature, 100 mA cm⁻² was loaded at full-cell and half-cell conditions. The voltage loss experiment was performed at 300 mA cm⁻² with a cell with high metal loading. The polarization resistance of the fuel cell increases with decreasing cell temperature, particularly at 30°C (Fig. 7). This is consistent with an abrupt increase in

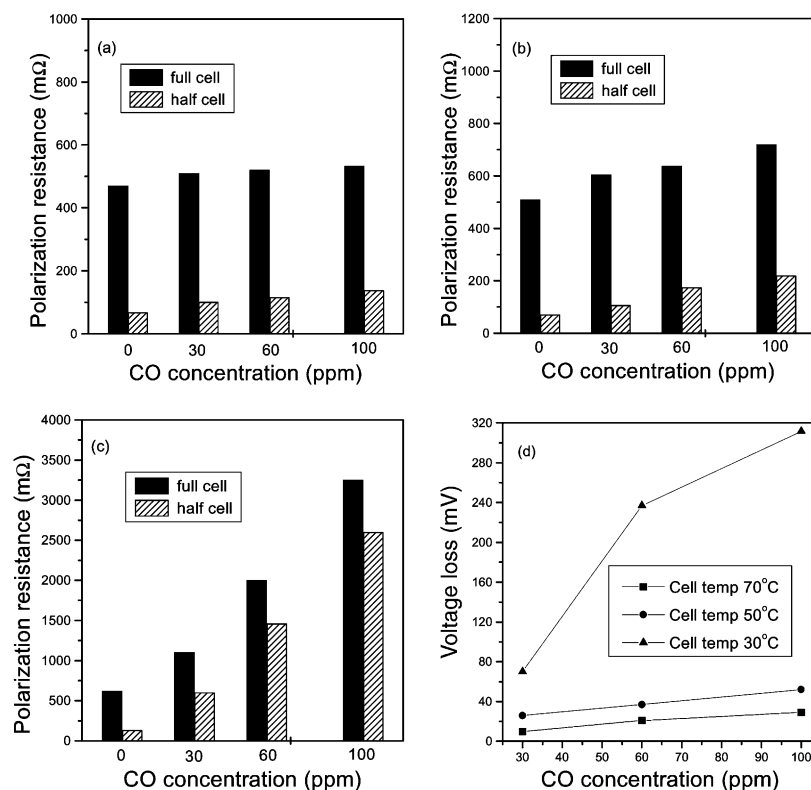


Fig. 7. Polarization resistance for full-cell and half-cell at current density of 100 mA cm⁻² and voltage loss: (a) 70°C; (b) 50°C; (c) 30°C; (d) voltage loss.

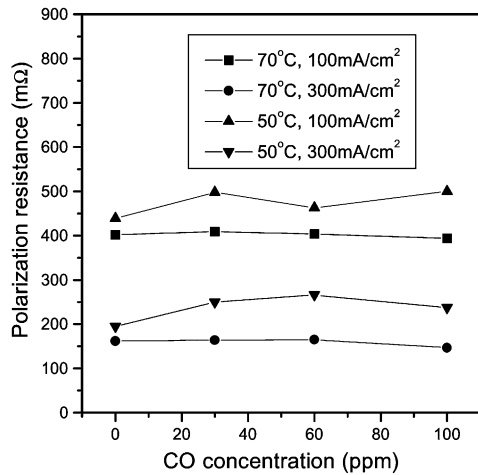


Fig. 8. Cathode polarization resistance as a function of CO concentration.

voltage loss at 30°C (Fig. 7(d)). The portion of the anode impedance is not large at cell temperatures of 70 and 50°C. Therefore, the impedance of the full-cell is mainly a cathode impedance. The portion of anode impedance does increase, however, with decrease in cell temperature. For 100 ppm CO, anode impedance increases from 25% (70°C) to 30% (50°C). The anode impedance increases greatly at a cell temperature of 30°C. As seen in Fig. 7, the impedance of a fuel cell at 0 ppm CO or high temperature is mainly a cathode impedance because the anode impedance is small. In the case of low temperature and high CO concentration, however, the impedance of the fuel cell is dependent on the anode side.

Next, we calculated the cathode polarization resistance. The effect of CO gas on the cathode can be seen in Fig. 8. The cathode polarization resistance changes little with increasing CO concentration. Also, the cathode polarization

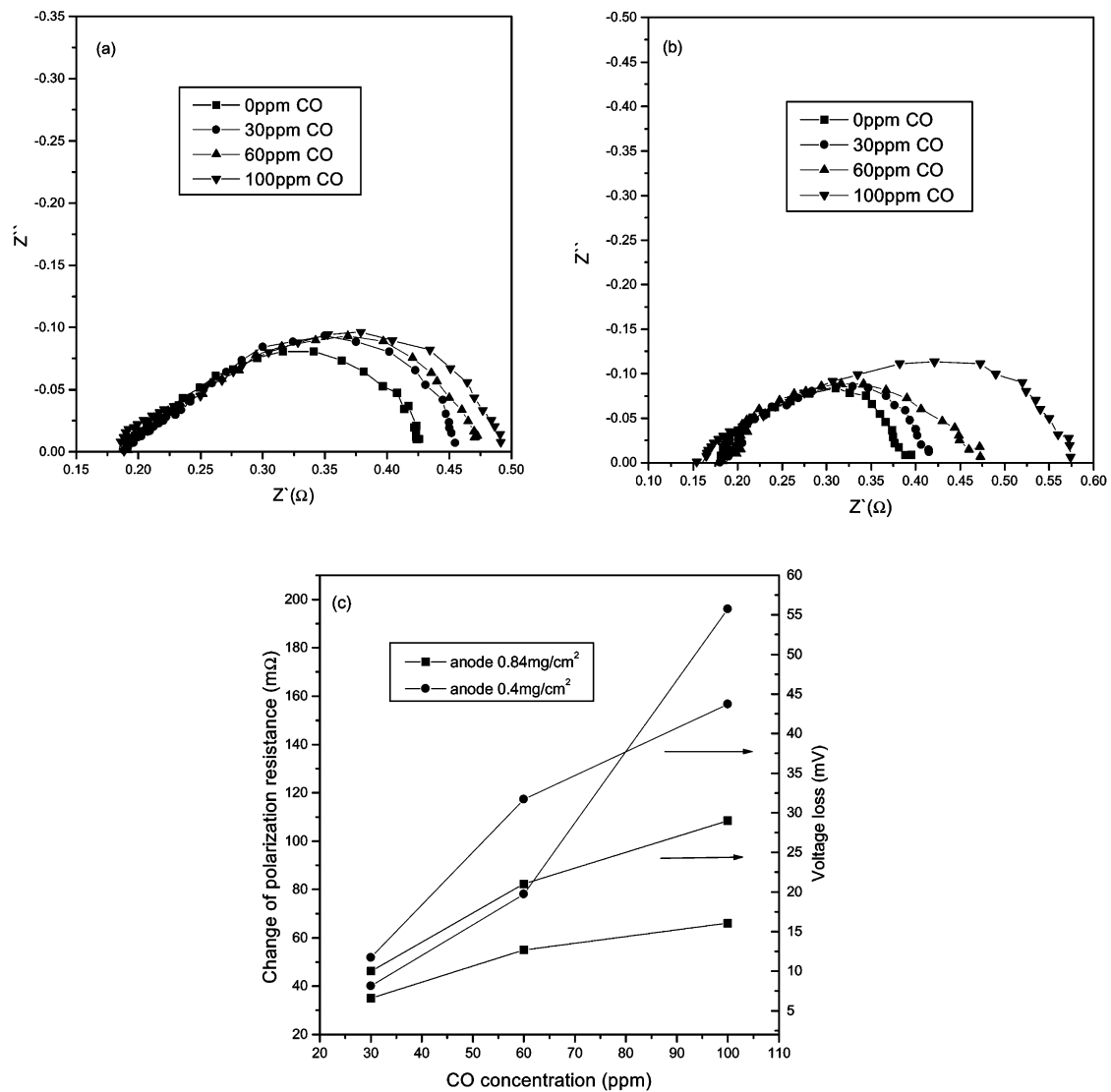


Fig. 9. Impedance spectra of full-cell with (a) high metal loading, (b) low metal loading, and (c) change of polarization resistance and voltage loss as a function of CO concentration at 70°C.

resistance decreases with increasing cell temperature and current density. It is also found from Fig. 8 that the CO gas is not very permeable through Nafion in the experimental range. This suggests that the CO gas has little effect on the cathode side.

The impedance spectra of the full-cell with various CO concentrations at a temperature of 70°C are presented in Fig. 9. The impedance measurements were performed at a current density of 300 mA cm⁻² for comparison with the voltage loss data given in Fig. 2. The impedance spectrum of a fuel cell with high metal loading and with a low metal loading is shown in Fig. 9(a) and (b), respectively. The impedance spectrum of the full-cell consists of cathode and anode impedance. As can be seen Fig. 7, a large portion of the impedance corresponds to the cathode impedance because the anode impedance is small. In Fig. 9, it is found that the polarization resistance increases with increasing CO concentration and the change of polarization resistance of a fuel cell with low metal loading is larger than that of one with high metal loading. Since the cathode is little influenced by CO concentration, this change of polarization resistance in a full-cell is due to an increase in anode impedance.

4. Conclusions

The effects of CO gas and anode-metal loading on H₂ oxidation in a PEMFC are investigated by ac impedance spectroscopy and voltage loss measurements. As the CO concentration increases, the voltage loss increases and is smaller for a fuel cell with high metal loading than one with a low metal loading because of vacant active sites. The polarization resistance of the charge-transfer reaction (high-frequency arc) and hydrogen dissociative chemisorption (medium-frequency arc) increase with increasing CO concentration. The gas-phase diffusion (low-frequency arc) is almost independent on CO concentration. The polarization resistances for charge-transfer and hydrogen dissociative chemisorption in a fuel cell with low metal loading are

larger than that in one with high metal loading, and increase greatly with increasing CO concentration. At high temperature, the cathode impedance is the main part because the anode impedance is small. At low temperature and high CO concentration, the impedance of a full-cell depends on the anode impedance. It is found that CO gas has little effect on cathode impedance.

Acknowledgements

This research has been supported by the High-Tech Research Center (Ministry of Education, Science, Sports and Culture, Japan) Project on Research and Development of Environmentally Friendly Energy.

References

- [1] R. Lemons, *J. Power Sources* 29 (1990) 251.
- [2] X. Ren, M.S. Wilson, S. Gottesfeld, *J. Electrochem. Soc.* 143 (1996) L12.
- [3] V.M. Schmidt, P. Brockerhoff, B. Hohlein, R. Menzer, U. Stimming, *J. Power Sources* 49 (1994) 299.
- [4] B. Hohlein, M. Boe, J. Bogild Hansen, P. Brockerhoff, G. Colmann, B. Emonts, R. Menzer, E. Riedel, *J. Power Sources* 61 (1996) 143.
- [5] T.J. Schmidt, H.A. Gasteiger, R.J. Behm, *J. Electrochem. Soc.* 146 (1999) 1296.
- [6] H.A. Gasteiger, N. Markovic, P.N. Ross, E.J. Cairns, *J. Phys. Chem.* 98 (1994) 617.
- [7] J. Divisek, H.F. Oetjen, V. Peinecke, V.M. Schmidt, U. Stimming, *Electrochim. Acta* 43 (1998) 3811.
- [8] M. Gotz, H. Wendt, *Electrochim. Acta* 43 (1998) 3637.
- [9] H.F. Oetjen, V.M. Schmidt, U. Stimming, F. Trila, *J. Electrochem. Soc.* 143 (1996) 3838.
- [10] G. Sandstede (Ed.), *From Electrocatalysis to Fuel Cells*, University of Washington Press, Seattle/London, 1997, p. 1.
- [11] P.K. Shen, A.C.C. Tseung, *J. Electrochem. Soc.* 141 (1994) 3082.
- [12] J.T. Mueller, P.M. Urban, *J. Power Sources* 75 (1998) 139.
- [13] M. Ciureanu, H. Wang, *J. Electrochem. Soc.* 146 (1999) 4031.
- [14] R.J. Bellows, E.P. Marucchi-Soos, Terence Buckley, *Ind. Eng. Chem. Res.* 35 (1996) 1235.
- [15] W. Vogel, J. lundquist, P. Ross, P. Stonehart, *Electrochim. Acta* 20 (1975) 79.